RAPID COMMUNICATIONS

PHYSICAL REVIEW B VOLUME 51, NUMBER 7 15 FEBRUARY 1995-I

Electron–acoustic-phonon scattering rates in cylindrical quantum wires

SeGi Yu* and K. W. Kim
Department of Electrical and Computer Engineering, North Carolina State University, Raleigh, North Carolina 27695-7911

Michael A. Stroscio and G. J. Iafrate
U.S. Army Research Office, P.O. Box 12211, Research Triangle Park, North Carolina 27709-2211
(Received 1 December 1994)

The electron–acoustic-phonon scattering rates in a cylindrical quantum wire are studied. Considering the quantum wire as an elastic continuum, the confined-phonon dispersion relation is calculated for two cardinal boundary conditions: free-surface and clamped-surface boundary conditions. The scattering rates due to the deformation-potential interaction are obtained for these two confined phonons and are compared with those of bulklike phonons. The results show that the inclusion of acoustic-phonon confinement effects may be crucial for calculating accurate low-energy-electron scattering rates in nanostructures. It is also demonstrated that the anisotropy should not be ignored for materials of cubic symmetry.

Proposed applications of mesoscopic electronic structures involve carrier transport at low temperatures and low carrier energies. In many cases, the regime of interest is one where dimensional confinement modifies the phase space substantially. In this low-temperature, low-energy regime,[1–7] acoustic phonons play an enhanced role in carrier scattering and may dominate over the scattering of carriers by optical phonons. Furthermore, in nanoscale structures it is possible that phase-space restrictions may weaken or forbid optical-phonon scattering processes that would normally dominate in bulk structures. In recent years, there has been an extensive literature on the role of dimensional confinement in modifying longitudinal-optical phonon modes and their interactions with charge carriers in nanoscale and mesoscopic semiconductor structures (see, for example, Refs. 8–10, and the numerous papers referenced therein); however, there are relatively few treatments dealing with the role of dimensional confinement in modifying acoustic-phonon modes and their interactions with charge carriers.[1–3,11,12] In particular, few efforts have been reported that formulate a theory of the electron–acoustic-phonon interaction in nanoscale structures where the treatment of acoustic-phonon confinement effects may be essential.[13–15] The need for such theoretical treatments has been demonstrated recently by experimental studies[1–5,7,11] providing both direct and indirect evidence of the importance of acoustic-phonon confinement in reduced-dimensional electronic structures. In this paper, we present golden-rule scattering rates for the electron interaction with confined acoustic phonons in a mesoscopic quantum wire with cylindrical geometry. A quantized description of acoustic-phonon modes (developed under the elastic-continuum model) is used to formulate the deformation-potential Hamiltonian. As for the case of rectangular quantum wires,[14] it is found that a proper treatment of confined acoustic phonons in cylindrical quantum wires may be crucial to correctly model electron-scattering rates at low energies in nanoscale structures.

In the limit of long-wavelength acoustic phonons, it is sufficient to treat the material as an elastic continuum. A number of experiments confirm the usefulness of the continuum model in nanostructures.[3–5,7] A cylindrical quantum wire of infinite length in the z direction with radius a is assumed for materials of isotropic symmetry. In this paper, we consider only the longitudinal modes of the confined acoustic phonons since the dominant contribution to the electron–acoustic-phonon interaction through the deformation potential comes from these modes. These longitudinal modes are well established in an isotropic medium of a cylinder,[16] and the normalization of confined phonons and the deformation Hamiltonian have been reported previously in Ref. 15. The acoustic waves move in radial planes without an azimuthal angle dependence, and the displacements are given by

$$u_r(r,z)=\left[\frac{d}{dr}\{BJ_0(k_d r)+AJ_0(k_t r)\}\right]e^{i(kz-\omega t)}, \quad \text{(1a)}$$

$$u_z(r,z)=i\left[kBJ_0(k_d r)+\frac{-k_t^2}{k}AJ_0(k_t r)\right]e^{i(kz-\omega t)}, \quad \text{(1b)}$$

where J_0 and J_1 are the ordinary Bessel functions, A and B are constants to be determined later, ω is an angular frequency, and k is the z-component wave vector. In addition, k_d and k_t are represented as

$$k_{d,t}^2=\frac{\omega^2}{v_{d,t}^2}-k^2, \quad (2)$$

where v_d (v_t) is the longitudinal (transverse) velocity. The longitudinal waves are coupled modes of axial and radial modes that have the quantized wave vectors k_t and k_d, respectively. In a cylinder, these two partial waves are coupled to satisfy the boundary condition (BC) at the surface in a manner similar to that for Lamb waves in a free isotropic plate.[16]

The general BC's for the confined acoustic phonons are that the displacement ($\vec{u}$) and the normal components of stress ($\vec{\vec{T}}\cdot\hat{n}$), or the tractional force, are continuous across surfaces where the elastic properties change discontinuously. For simple cases, there are two cardinal BC's: the free-

surface BC (FSBC) and the clamped-surface BC (CSBC). The free surface is a boundary between an elastic material and vacuum where the normal components of the stress tensor are zero and the displacement is unrestricted. The clamped surface is a boundary between an elastic material and a perfectly rigid material where the displacement is zero and the normal components of the stress tensor are unrestricted. Although most quantum wires are not surrounded by vacuum or by an extraordinarily hard material, the use of these two cardinal BC's is employed frequently in classical acoustics for cases where analytical solutions are hard to find. Furthermore, the calculation for the FSBC case may be applied to free-standing quantum wires fabricated by lateral etching techniques. As a result, we have adopted these two BC's to investigate the electron–acoustic-phonon interaction in the present paper.

The dispersion relations of confined phonons and the constant ratios $\beta=B/A$ are obtained from the BC's. The dispersion relation for confined phonons with the FSBC is

$$(k^2-k_t^2)^2\frac{(k_da)J_0(k_da)}{J_1(k_da)}-2k_d^2(k^2+k_t^2)+4k^2k_d^2\frac{(k_ta)J_0(k_ta)}{J_1(k_ta)}=0, \quad (3)$$

and that for phonons with the CSBC is

$$k_d^2\frac{(k_ta)J_0(k_ta)}{J_1(k_ta)}+k^2\frac{(k_da)J_0(k_da)}{J_1(k_da)}=0. \quad (4)$$

(On the other hand, the bulklike phonons are dispersionless; i.e., phase velocity is constant with respect to the wave vector.) The constant ratios for β are given by

$$\beta=-\frac{k_t(k^2-k_t^2)}{2k^2k_d}\frac{J_1(k_ta)}{J_1(k_da)}$$

for FSBC and

$$\beta=\frac{k_t^2}{k^2}\frac{J_0(k_ta)}{J_0(k_da)}$$

for CSBC. The individual values of A and B are determined by phonon normalization.[15]

The Hamiltonian describing the deformation-potential interaction for the electron and the acoustic phonon is expressed such that $H_{\rm def}=-E_a\vec{\nabla}\cdot\vec{u}$, where E_a is the deformation-potential constant. Hence, in the confined phonon case the longitudinal modes are more important than torsional and flexural modes as discussed before. In the bulklike phonon case, only the modes vibrating parallel to the propagation direction contribute to the scattering rates, and accordingly the transverse velocity does not appear. The electrons confined in a cylindrical quantum wire are assumed to be the ground state in the extreme quantum limit. Finally, the scattering rates for the deformation potential are calculated using standard procedures and assuming the Fermi golden rule.

Although it is mathematically easy to treat acoustic waves in an isotropic material, there are few materials of isotropic symmetry. Furthermore, the symmetry of most semiconductor materials of interest is not isotropic but cubic. The acoustic waves in these materials may be determined directly for the case of the cubic symmetry or through proper analysis under the assumption that the material is isotropic. The acoustic-wave equation, or Christoffel equation, for the cylinder may be solved by the first approach, but there is great complexity due to the extra elastic constant that prevents one from extracting any information from the algebraic results. Accordingly, we follow the second method and analyze a range of solutions. Due to the potential technological importance of the GaAs quantum wire, calculations are confined to the case of GaAs that has cubic symmetry. This calculation can be extended to other materials of cubic symmetry without difficulty.

In isotropic materials, the slowness curve, or the inverse-velocity curve, which gives the magnitude of $\vec{k}/\omega$ as a function of its direction, consists of two concentric circles independent of the acoustic-wave-propagation characteristics.[16] On the other hand, the slowness curve for materials of cubic symmetry is more complicated than that for isotropic materials. But for the case of some special directions, the curve takes a simple form. For the propagation along any crystal axis, the curve is represented by two concentric circles that represent the pure shear wave and the pure longitudinal wave as for isotropic materials. As a result, it is possible to employ the isotropic assumption for GaAs as long as we consider propagation in the [001] direction; i.e., the case that one of the crystal axes coincides with the z direction. This is the condition we consider throughout the calculation.

Two different parameter sets are applied in order to determine the effect of the anisotropy of GaAs as well as to quantify the range of possible deformation-potential scattering rates for cylindrical quantum wires. The first set, denoted as PS1, is chosen such that the experimentally determined v_d and Poisson ratio σ fix the value of v_t from the isotropic assumption (PS1: $v_d=4.78\times10^5$ cm/sec, $v_t=2.56\times10^5$ cm/sec, $\sigma=0.33$).[17] The second set is obtained by taking v_d and v_t as the velocities of GaAs [001] propagating acoustic waves; these velocities yield a value for σ (PS2: $v_d=4.78\times10^5$ cm/sec, $v_t=3.35\times10^5$ cm/sec, $\sigma=0.018$). For both sets, the deformation-potential constant E_a and the lattice temperature are assumed to be 7.8 eV and 77 K, respectively, and five lowest modes are considered.

The scattering rates for the deformation-potential interaction of the electron with the FSBC (PS1, PS2) and the bulklike phonons are plotted in Fig. 1 as functions of electron energy. The important fact is that the FSBC scattering rates are very sensitive to the velocity of the confined phonon. The scattering rates corresponding to the PS1 and PS2 parameter sets differ substantially; indeed, the difference amounts to several orders of magnitude in the low-electron-energy region. This difference is due mainly to the different transverse velocities. To investigate the dependence of the scattering rate on velocity further, we have also considered other parameter sets that take the same values of PS1 except the value of v_t. The value of v_t is changed continuously from that of PS1 to that of PS2. In these cases, the scattering rates increase continuously with the increase in the value v_t. In particular, the enhancement is especially strong in the low-electron-energy region. The scattering rates with v_t having the value of PS2 are much higher than for PS1, and are very similar to those of the PS2 case. This finding is in striking

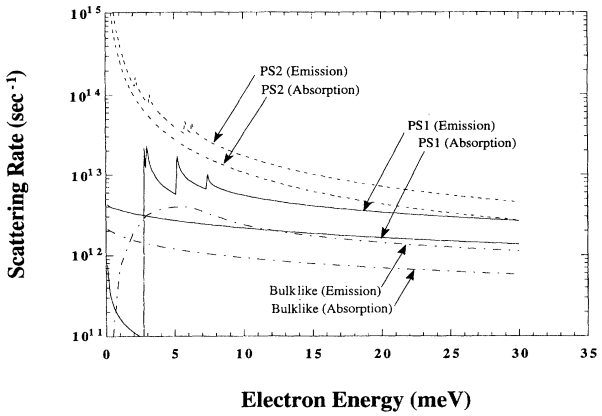

FIG. 1. Scattering rates for the deformation-potential interaction of electrons with the FSBC confined acoustic phonons (PS1, PS2) and bulklike phonons in a cylindrical GaAs quantum wire (radius of 22.6 Å) at 77 K as a function of electron energy. Solid (dashed) lines are for the PS1 (PS2), and dashed-dotted lines are for the bulklike phonons. The plotting resolution depicted is not fine enough to illustrate fully the importance of the density-of-states effects in the quantum wire.

contrast to the case of PS1 considering that those two differ only in the value of v_t. A careful analysis reveals that the difference in the scattering rates (and, subsequently, the dependence on v_t) is associated with the lowest-phonon branch. As shown in Fig. 2, the lowest mode for the confined phonons with the FSBC has no cutoff frequency unlike the cases for the other higher modes. Hence the quantized wave vector k_t, defined in Eq. (2), of this lowest mode is very sensitive to the choice of v_t while the other are not. The magnitude of λ_t $(=2\pi/k_t)$, which corresponds to the characteristic wavelength of the axial partial wave, is a measure of the phonon amplitude. Since the deformation Hamiltonian is proportional to phonon amplitude, large values of λ_t, i.e.,

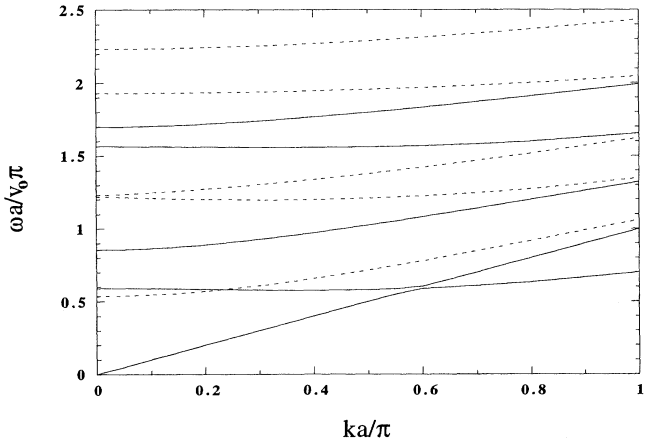

FIG. 2. Dispersion relation of the five lowest confined acoustic photons with the FSBC (solid lines) and the CSBC (dashed lines) in a cylindrical GaAs quantum wire. The value of the Poisson ratio σ is 0.018 and v_0 represents the sound velocity of Young's module mode.

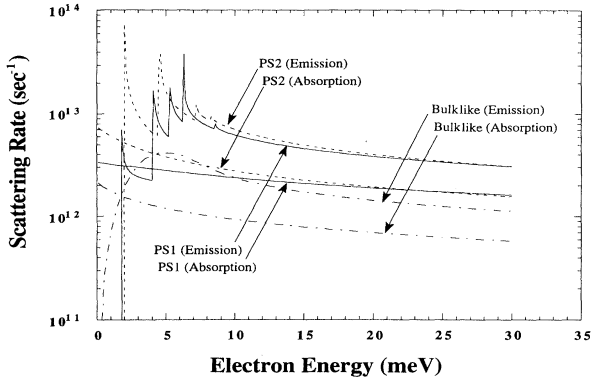

FIG. 3. Scattering rates for the deformation-potential interaction of electrons with the CSBC confined acoustic phonons (PS1, PS2) and bulklike phonons in a cylindrical quantum wire (radius of 22.6 Å) at 77 K as a function of electron energy. Solid (dashed) lines are for the PS1 (PS2), and dashed-dotted lines are for the bulklike phonons. As in Fig. 1, the plotting resolution is limited.

small k_t (or large v_t), imply large scattering rates for the deformation potential. Thus, the scattering rates are strongly affected by acoustic-phonon velocity; consequently, the electron-phonon scattering rate in a GaAs quantum wire is highly dependent on the direction of the phonon propagation due to the anisotropy of GaAs.

Figure 3 depicts the scattering rate for the case of confined phonons with the CSBC; this plot exhibits smaller scattering rates in comparison with the case of the FSBC. The relatively small scattering rates are expected from the inspection in the functional form of the displacement. Since the CSBC requires the displacement at the boundary to be zero, the displacement of the lowest mode has maximum value at the center of the cylinder while its derivative (or divergence) is very small. This small divergence of the phonon displacement makes the electron-phonon coupling small since the electron's ground-state wave function has its maximum at the center. At the same time, the acoustic phonons with the CSBC generally have higher energies than those with the FSBC since every CSBC acoustic phonon has a cutoff frequency as shown in Fig. 2. It is difficult for the electron to emit or absorb phonons with higher energies. As a result, the relatively high energy characteristics of phonons and the small electron-phonon coupling make the scattering rate for the CSBC smaller than that for the FSBC. Another interesting point to note with the CSBC is a weak dependence on phonon velocity due to the existence of cutoff frequencies, as in the case of higher modes with the FSBC. From Figs. 1 and 3 it can be concluded that confined phonons (both with the FSBC and the CSBC) exhibit larger scattering rates than for the bulklike phonon case. Particularly in the low-electron-energy region, confined phonons exhibit much larger values as well as several peaks reflecting the characteristics of the one-dimensional density of state. Besides the large differences in values of scattering rates, the deformation-potential Hamiltonian for the bulklike phonon does not include the dependence on transverse velocity, which may have an important role in anisotropic materials.

Finally, in Fig. 4, we compare the scattering rates for a cylindrical and a rectangular wire. In the cylindrical wire

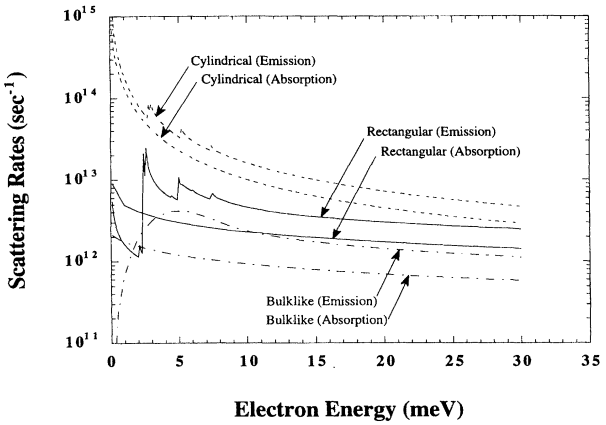

FIG. 4. Scattering rates for the deformation-potential interaction of electrons with the confined acoustic phonons in a cylindrical (dashed line) and a rectangular GaAs quantum wire (solid line). An identical cross section is chosen for the two wires (cylindrical wire of radius 22.6 Å, rectangular wire of 28.3×56.6 Å^2) and the values of parameters are the same as in Ref. 14. In the cylindrical wire confined phonons with FSBC are used, and the separable solutions for confined phonons are adopted for the rectangular wire as discussed in Ref. 14. For comparison, the rate with the bulklike phonons for the cylindrical wire is also plotted (dashed-dotted line). As in Figs. 1 and 3, the plotting resolution is limited.

confined phonons with FSBC are used, and an approximate solution as described in Ref. 14 is adopted for the rectangular geometry. The values of the parameters are taken to be those used in Ref. 14 ($v_d=4.78\times10^5$ cm/sec, $v_t=3.35\times10^5$ cm/sec, $\sigma=0.33$). When comparing two wires having a same cross-sectional area (cylindrical wire of radius 22.6 Å, rectangular wire of 28.3×56.6 Å^2), we find that there is a resemblance between the scattering rates for these two wires. Since the scattering rates for the rectangular and the cylindrical wires using bulklike phonons are very close, only the cylindrical-wire case is plotted to facilitate clear presentation of the results. The nearly identical scattering rates for the bulklike phonons can be easily understood, considering that the coupling between the electrons and the bulklike phonons are essentially the same in these two wires with the same cross-sectional area. For the confined acoustic phonons, the cylindrical wire exhibits considerably larger scattering rates than the corresponding rectangular wire. Aside from the difference in the functional form of the electron-phonon coupling (i.e., the difference in electron and phonon envelope functions), the gap in the magnitudes of the scattering rates between the cylindrical wire and the rectangular wire may be at least partly due to the incompleteness of the separable solutions used in the rectangular wire. However, the overall similarity between the rates obtained in two wires demonstrates the fact that the approximate theory developed previously for a rectangular wire[14] may be considered a valuable guideline for calculating the scattering rates in such a geometry, where an exact analytical solution does not exist.

In conclusion, we have calculated the scattering rates for the electron and several kinds of confined acoustic phonons through the deformation-potential interaction in a cylindrical quantum wire. It is found that confined phonons produce larger scattering rates than the bulklike phonons, and the scattering rates are highly dependent on the phonon propagation velocity. In addition to its relatively small scattering rates, the use of bulklike phonons in calculating electron–acoustic-phonon scattering rates may be flawed due to the neglect of anisotropic dependence on transverse velocity, which is of potential significance in many semiconductor materials and nanostructures.

The authors acknowledge many helpful discussions with Dr. A. Ballato and Professor V. Mitin. This work was supported, in part, by the Office of Naval Research and the U.S. Army Research Office.

*Also at Department of Physics, North Carolina State University, Raleigh, NC 27695-8202.

[1] B. Hillebrands, S. Lee, G. I. Stegeman, H. Cheng, J. E. Potts, and F. Nizzoli, Phys. Rev. Lett. **60**, 832 (1988).

[2] J. Seyler and M. N. Wybourne, Phys. Rev. Lett. **69**, 1427 (1992).

[3] Z. V. Popvic, J. Spitzer, T. Ruf, M. Cardona, R. Notzel, and K. Ploog, Phys. Rev. B **48**, 1659 (1993).

[4] R. Bhadra, M. Grimsditch, I. K. Schuller, and F. Nizzoli, Phys. Rev. B **39**, 12 456 (1989).

[5] M. Grimsditch, R. Bhadra, and I. K. Schuller, Phys. Rev. Lett. **58**, 1216 (1987).

[6] P. V. Santos, A. K. Sood, M. Cardona, K. Ploog, Y. Ohmori, and H. Okamoto, Phys. Rev. B **37**, 6381 (1988).

[7] A. Tanaka, S. Onari, and T. Arai, Phys. Rev. B **47**, 1237 (1993).

[8] N. Mori and T. Ando, Phys. Rev. B **40**, 6175 (1989).

[9] H. Rücker, E. Molinari, and P. Lugli, Phys. Rev. B **45**, 6747 (1992).

[10] M. A. Stroscio, G. J. Iafrate, K. W. Kim, M. A. Littlejohn, A. R. Bhatt, and M. Dutta, in *Integrated Optics and Optoelectronic*, edited by K.-K. Wong and M. Razeghi (SPIE, Bellingham, WA, 1993), Vol. CR45, p. 341.

[11] H. Benistry, C. M. Sotomayor-Torrés, and C. Weisbuch, Phys. Rev. B **44**, 10 945 (1991).

[12] N. Nishiguchi, Phys. Rev. B **50**, 10 970 (1994).

[13] N. Bannov, V. Mitin, and M. A. Stroscio, Phys. Status Solidi B **183**, 131 (1994).

[14] S. Yu, K. W. Kim, M. A. Stroscio, G. J. Iafrate, and A. Ballato, Phys. Rev. B **50**, 1733 (1994).

[15] M. A. Stroscio, K. W. Kim, S. Yu, and A. Ballato, J. Appl. Phys. **76**, 4670 (1994).

[16] B. A. Auld, *Acoustic Fields and Waves* (Wiley, New York, 1973).

[17] J. S. Blakemore, J. Appl. Phys. **53**, R123 (1982).